




Article

Comparative Study of Phase Transformation in Single-Crystal Germanium during Single and Cyclic Nanoindentation

Koji Kosai , Hu Huang  and Jiwang Yan * 

Department of Mechanical Engineering, Faculty of Science and Technology, Keio University, Yokohama 2238522, Japan; koji.kosai@keio.jp (K.K.); huanghuzy@163.com (H.H.)

* Correspondence: yan@mech.keio.ac.jp; Tel.: +81-45-566-1445

Academic Editor: Ronald W. Armstrong, Stephen M. Walley and Wayne L. Elban

Received: 30 September 2017; Accepted: 30 October 2017; Published: 1 November 2017

Abstract: Single-crystal germanium is a semiconductor material which shows complicated phase transformation under high pressure. In this study, new insight into the phase transformation of diamond-cubic germanium (dc-Ge) was attempted by controlled cyclic nanoindentation combined with Raman spectroscopic analysis. Phase transformation from dc-Ge to rhombohedral phase (r8-Ge) was experimentally confirmed for both single and cyclic nanoindentation under high loading/unloading rates. However, compared to single indentation, double cyclic indentation with a low holding load between the cycles caused more frequent phase transformation events. Double cyclic indentation caused more stress in Ge than single indentation and increased the possibility of phase transformation. With increase in the holding load, the number of phase transformation events decreased and finally became less than that under single indentation. This phenomenon was possibly caused by defect nucleation and shear accumulation during the holding process, which were promoted by a high holding load. The defect nucleation suppressed the phase transformation from dc-Ge to r8-Ge, and shear accumulation led to another phase transformation pathway, respectively. A high holding load promoted these two phenomena, and thus decreased the possibility of phase transformation from dc-Ge to r8-Ge.

Keywords: single crystal; germanium; nanoindentation; phase transformation; crystal defect; cyclic load

1. Introduction

Pressure-induced formation of various metastable polymorphs takes place in single-crystal germanium (Ge) during diamond anvil cell (DAC) and nanoindentation tests. Previous studies reported that diamond cubic Ge (dc-Ge) transforms to metallic (β -Sn)-Ge at a pressure of ~ 10 GPa [1–4]. When the pressure releases, this metallic phase transforms to various metastable structures depending on the experimental conditions, such as simple tetragonal phase (st12-Ge) [5–8], rhombohedral phase (r8-Ge) [6,7,9,10], body centered cubic phase (bc8-Ge) [5,6,11], as well as amorphous Ge (a-Ge) and dc-Ge as end phases [8,11]. Another phase of hexagonal diamond Ge (hd-Ge) is also confirmed by compression of a-Ge [9,12,13].

These polymorphs possess very different characteristics from their lowest energy structures, which may open up new applications in future microelectronics and photovoltaics. For this purpose, the complicated phase transformation process of Ge has been widely investigated. For example, in the DAC experiment by Nelmes et al., decompression speed was found to be critical for phase transformation, i.e., slow decompression caused phase transformation to st12-Ge while fast decompression promoted phase transformation to bc8-Ge [5]. Some other studies by nanoindentation on dc-Ge reported more

complicated responses against pressure [8,10,11,14]. Slow indentation with a spherical indenter could induce no phase transformation but only plastic deformation by formation of twinning and dislocation slip [8,10,14] which prevented phase transformation by stress release. However, when using a sharp indenter tip, this kind of defect nucleation was suppressed and phase transformations were confirmed [11]. Extremely fast indentation resulted in formation of st12-Ge [8], and low temperature led to formation of r8-Ge or a-Ge [10]. Investigation of the phase transformation in a-Ge was also performed via indentation [14–17] in which phase transformations can be induced easily compared with dc-Ge because of higher resistance of a-Ge against deformation by slip and twinning. According to the results of indentation on a-Ge, two clear phase transformation pathways via (β -Sn)-Ge have been established [14]. The authors stated that the intermediate (β -Sn)-Ge may transform to two end phases depending on whether the transforming region is constrained or not. Unconstrained (β -Sn)-Ge transforms to dc-Ge with possible trace of st12-Ge while the constrained one undergoes a phase transformation to unstable r8-Ge and finally hd-Ge. They mentioned that both of these two types of phase transformation could occur in the same indent for dc-Ge. The same research team also studied phase transformation behaviors of crystalline Ge by DAC experiment [7]. They classified phase transformations of (β -Sn)-Ge on unloading depending on hydrostaticity. Namely, quasihydrostatic conditions resulted in formation of r8-Ge while the presence of shear led to nucleation of st12-Ge. Their findings were consistent with previously reported phase transformations and helpful to explain the detailed mechanisms [7,14].

Even though the basic phase transformation process of Ge has been classified using a-Ge, it is still important to study and explain dominant phase transformation behaviors of dc-Ge because of the complexity of pressure-induced behaviors [14]. For Si, which has the same crystal structure as Ge, similar pressure-induced phase transformations have been widely reported [1–4,6,18–29], and some new insights into the phase transformation behaviors were further revealed by a multi cyclic nanoindentation method [20–24]. In this current paper, nanoindentation responses of single-crystal Ge under single and double cyclic nanoindentation tests were comparatively investigated. Combined with Raman analysis of residual phases in indents, a dominant phase transformation pathway of dc-Ge under repetitive pressure was established, which may open up new insights into pressure-induced phase transformations of crystalline Ge.

2. Experimental Details

A dc-Ge (111) wafer with thickness of 0.9 mm was used for experiments. Nanoindentation tests were performed on an ENT-1100a nanoindentation instrument (Elionix Inc., Tokyo, Japan) equipped with a Berkovich diamond indenter. In this experiment, single and double cyclic nanoindentation tests were carried out according to the protocol as shown in Figure 1 and the parameters in Table 1. Firstly, the indentation load increased to 50 mN under a given loading rate, held for one second, and then decreased under the same unloading rate as loading rate. For comparison, various loading/unloading rates—10, 25, or 50 mN/s—were used. For the single mode, the indentation load returned to 0 mN and then the test finished, while for the double mode, unloading stopped at a controlled residual load (ΔP) and then held for a given load holding time (LHT). As listed in Table 1, ΔP was varied from 0 to 14 mN with LHT of 5 s. Nanoindentation tests with LHT of 20 s were also conducted under $\Delta P = 2$ mN for comparison. After LHT, the second cycle indentation progressed with the same process as single mode from ΔP . For each experimental condition, 20 nanoindentation tests were performed to ensure the reliability of the results.

Residual phases of the all indents were measured by the NRS-3000 Raman micro-spectrometer (JASCO, Tokyo, Japan) with a 532 nm wavelength laser focused to a ~ 1 μm spot size. To ensure that the residual phases were minimally affected by further phase transformation at room temperature [5,11,13], the measurement of residual phases in indents was performed within three hours after indentation. In previous studies, some specific deformation responses, for example pop-in, pop-out, and elbow have been reported in indentation studies of Si [20–28] and Ge [8,10,11,14–16,23]. In this study, the effects of

experimental parameters on these deformation responses were statistically analyzed as well as phase transformation process during both single and cyclic indentation.

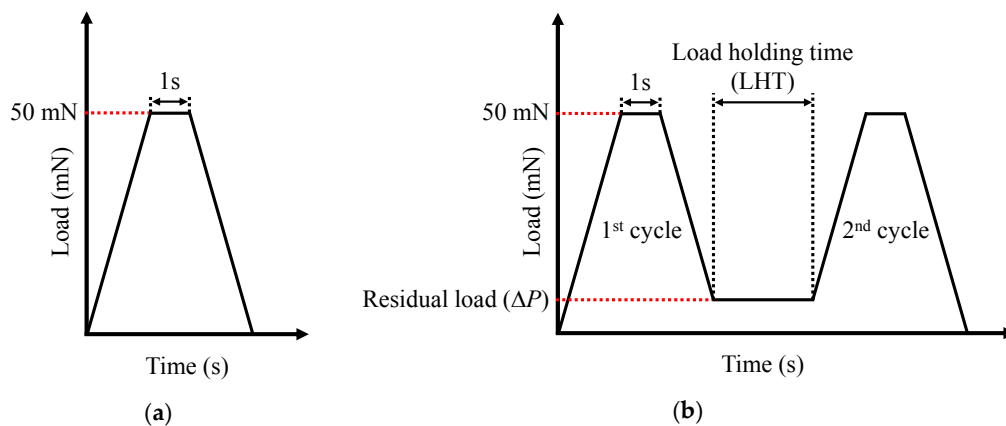


Figure 1. Nanoindentation experimental protocols: (a) single mode; (b) double cyclic mode.

Table 1. Experimental parameters for each indentation mode.

Indentation Mode	Maximum Load (mN)	Loading/Unloading Rate (mN/s)	ΔP (mN)	Length of LHT (s)
Single	50	10, 25, 50	-	-
Double cyclic	50	10, 25, 50	0, 2, 6, 10, 14	5 (or 20 for $\Delta P = 2$ mN)

3. Results and Discussions

3.1. Correlation between Specific Deformation Responses during Nanoindentation Tests and Phase Transformation Behaviors

Figure 2 illustrates typical load-displacement curves obtained under single and double cyclic nanoindentation tests, with shift of the second cycle curves in double cyclic nanoindentation for clarity. For both testing modes, pop-in events marked by arrows in Figure 2 are observed during the loading process under various loading/unloading rates. This event was reported as a result of slip generation in dc-Ge sample and/or phase transformation to $(\beta\text{-Sn})\text{-Ge}$ [10,14]. In addition to the pop-in event during loading, unloading also showed some specific deformation events, i.e., pop-out and elbow as illustrated in Figure 3. The correlation between these events and phase transformation has been established for indentation of Si [23–28] and cold indentation of Ge [10]. At room temperature, ultra-fast indentation of dc-Ge also triggered these phenomena [8], but the correspondence of these events with phase transformation was not clearly addressed. Thus, the correlation between these events and phase transformation behavior will be further discussed later in this section.

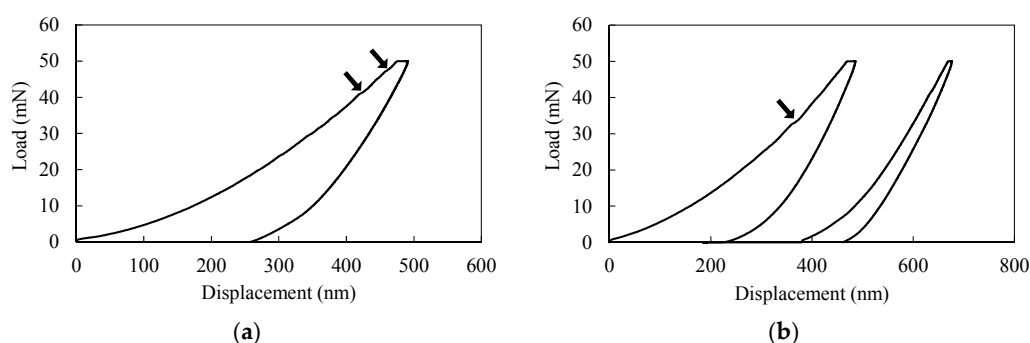


Figure 2. Cont.

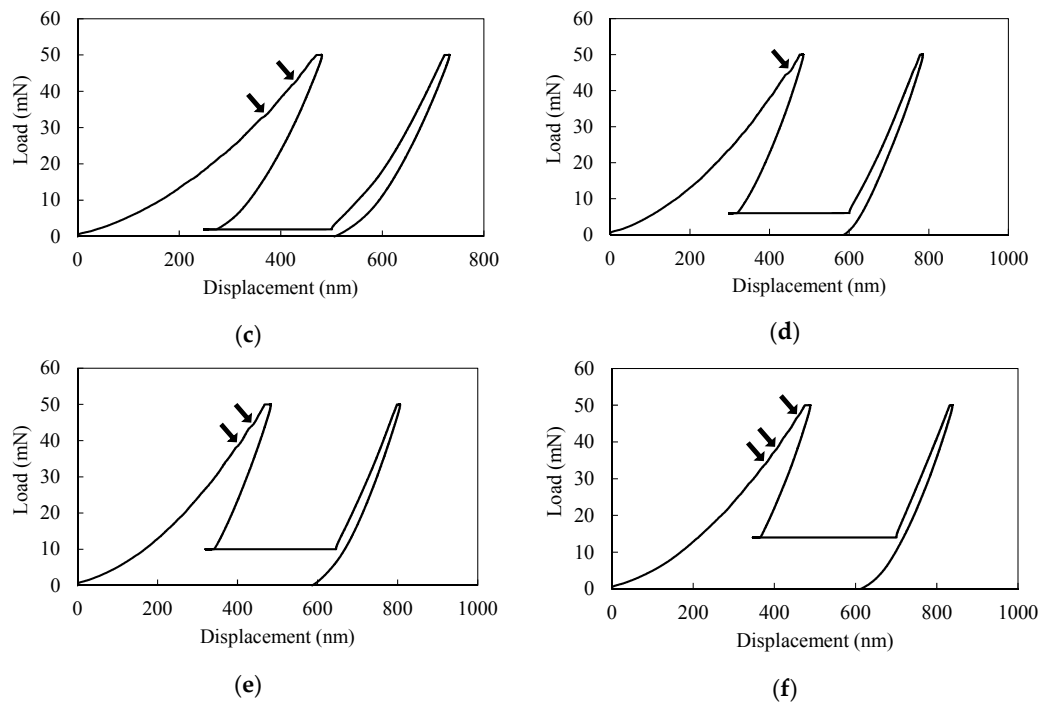


Figure 2. Load-displacement curves obtained by each mode of indentation under loading/unloading rate of 50 mN/s and LHT = 5 s: (a) single; (b) double, $\Delta P = 0$ mN (no residual load); (c) double, $\Delta P = 2$ mN; (d) double, $\Delta P = 6$ mN; (e) double, $\Delta P = 10$ mN; (f) double, $\Delta P = 14$ mN: all graphs of double cyclic indentation include artificial shift between cycles (arrows indicate pop-in events).

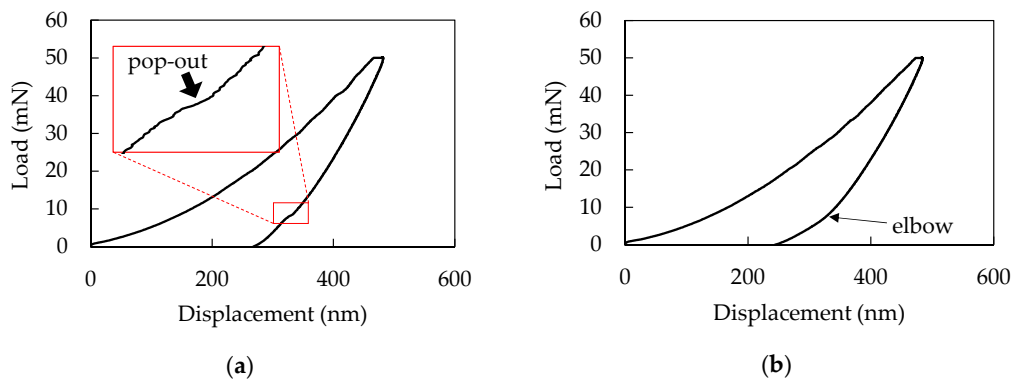


Figure 3. Specific deformation in unloading process: (a) pop-out; (b) elbow (single, loading/unloading rate of 50 mN/s).

Figure 4 illustrates Raman spectra obtained from residual indents, corresponding to the cyclic nanoindentation experiments in Figure 2. Compared with the main peak of pristine dc-Ge at 301 cm^{-1} , the corresponding peaks obtained from the indents show a little higher wavenumber as a result of compressive stress [14,23]. Furthermore, a broad component below 290 cm^{-1} corresponding to a-Ge and some peaks around 203, 225, and 247 cm^{-1} corresponding to r8-Ge phases [6,9,10,14] are observed. Bc8-Ge also shows very similar peaks to those of r8-Ge [6,11] and thus, it is difficult to distinguish these two phases from Raman data [9]. However, some recent studies indicated that the phase transformation from (β -Sn)-Ge to r8-Ge was dominant [9,14]. Accordingly, it can be concluded that the dominant transformed phase shown in Figure 4 is r8-Ge. Figure 5 presents the detection fraction of r8-Ge for every 20 indents under two loading/unloading rates of 25 and 50 mN/s with a same LHT of 5 s. For the loading/unloading rate of 10 mN/s, phase transformation was not identified by Raman detection.

This is a little different from previous research where formation of bc8-Ge was confirmed under 5 mN/s indentation [11] and it might be because of different detection resolutions for the transformed phase by Raman spectrometry. If the phase transformed region is only a part of the indented region, it may be difficult to position exactly the Raman spot on the phase transformed region with 1 μm resolution and 1 μm laser spot. However, in Figure 5, it is clear that faster indentation promoted phase transformation compared with the slower case under all conditions. This is due to an increase in loading rate, where the critical load for defect nucleation also increases, thus phase transformation becomes the dominant mechanism rather than defect nucleation in a crystalline Ge sample [8].

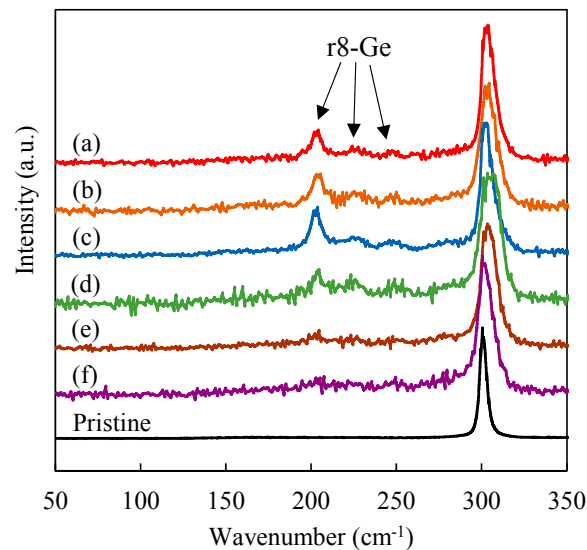


Figure 4. Raman spectra obtained from residual indents corresponding to the cyclic nanoindentation experiments in Figure 2.

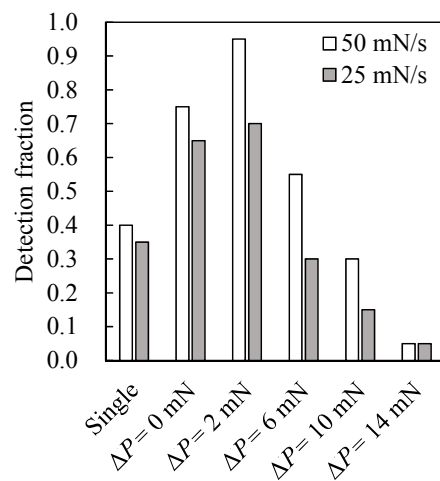


Figure 5. Detection fraction of r8-Ge under various experimental conditions (LHT = 5 s) (no detection under 10 mN/s).

Next, the correlation between the observed phase transformation to r8-Ge via (β -Sn)-Ge and the specific deformation events of pop-in, pop-out and elbow in this study will be discussed for the single indentation mode. For pop-in events, two mechanisms are suggested as the causes: slip generation in dc-Ge sample and/or phase transformation to (β -Sn)-Ge [10,14]. In this case, no correlation between r8-Ge formation and the pop-in events was confirmed, especially under the lowest loading/unloading rate of 10 mN/s which never caused phase transformation to r8-Ge in this study even though pop-in

events were frequently observed. Hence, the dominant cause of the observed pop-in events is expected to be defect nucleation rather than phase transformation. There is another possibility for the cause of pop-in events by phase transformation to intermediate (β -Sn)-Ge then ending up as dc-Ge, which was reported in indentation on a-Ge [14–17]. However, it is impossible to distinguish this possibility in our experiment because the end phase is the same as the initial phase.

The above discussion indicates that the pop-in events probably do not result from the phase transformation to (β -Sn)-Ge in this case. For an elbow on unloading, amorphization was reported as the reason [10,28], but it is difficult to assess the correlation between these two phenomena in this study because of the difficulty in judging the occurrence of amorphization which only showed a weak broad band on Raman spectra in this case. On the other hand, for pop-out events, the correlation exists that all indents with r8-Ge formation are accompanied with pop-out events, although some indents show only pop-out events without the observation of phase transformation to r8-Ge. In addition, faster loading/unloading rates promoted occurrence of pop-out events (13/20 for 50 mN/s; 11/20 for 25 mN/s; 4/20 for 10 mN/s) as well as phase transformation to r8-Ge as shown in Figure 5. These facts imply that the correlation between r8 phase formation and pop-out events exist as mentioned in studies of indentation of Si [23–28] and cold indentation on dc-Ge [10]. The appearance of pop-out events alone without phase transformation in some indents might result from insufficient resolution of the Raman spectrometer. Some other possibilities may still exist, for example, phase transformation to dc-Ge from (β -Sn)-Ge also affected the occurrence of pop-out events, but additional experiments with more detailed observations are required to distinguish the cause.

3.2. Effects of Indentation Modes on Phase Transformation Behaviors

Another clear tendency for the phase transformation behavior obtained from Figure 5 is that double cyclic indentation tests with lower residual load ΔP promoted the phase transformation to r8-Ge compared with single indentation. In the double cyclic indentation, r8-Ge was confirmed. Even though the correlation between phase transformation and pop-out events for the single mode was confirmed in Section 3.2, this kind of correlation did not exist for double cyclic indentation with low ΔP . In other words, phase transformation to r8-Ge was confirmed regardless of pop-out events in the double cyclic mode. On the other hand, the detection fraction decreases with increase in ΔP and finally becomes obviously lower than single indentation. This indicates that double cyclic indentation can promote phase transformation to r8-Ge, independent of pop-out response during unloading, although phase transformation is suppressed by high residual load ΔP . The effect of residual load on the formation of r8-Ge is further confirmed from the result of different LHT experiments shown in Figure 6. Even under a small ΔP of 2 mN, longer LHT increases the influence of residual load, showing a decreased detection fraction of r8-Ge.

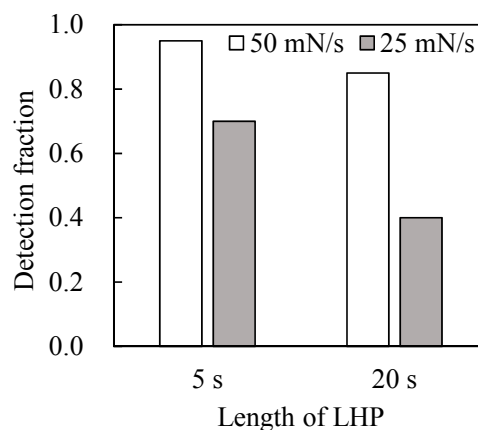


Figure 6. Detection fraction of r8-Ge under different LHT ($\Delta P = 2$ mN, loading/unloading rate of 50 mN/s).

The mechanism for promoting the formation of r8-Ge by multi cyclic nanoindentation can be explained by referring to a previous study on Si [20]. In that study, during multi cyclic nanoindentation, it was suggested that the transformed r8-Si/bc8-Si region expanded during subsequent cycles and finally a larger r8-Si/bc8-Si region was formed compared to single indentation [20]. This mechanism can be employed to this study. Namely, compared to single indentation, double cyclic indentation with small ΔP can expand the transformed region and result in a higher detection fraction of r8-Ge. The lower detection of r8-Ge under $\Delta P = 0$ mN compared with $\Delta P = 2$ mN is possibly caused by an error of noncontact between the indenter tip and sample surface. The case for $\Delta P = 0$ mN means that the load was completely removed from the sample, and the indenter tip might leave the sample surface. In such a case, friction might occur at the second contact and cause shear in the Ge sample, which could lead to phase transformation to dc-Ge or st12-Ge [7,14,17]. It should be noted that 1 of 20 indents with a residual load of 0 mN and loading/unloading rate of 50 mN/s has peaks around 195, 250, and 280 cm^{-1} corresponding to st12-Ge. The phase transformation caused by shear does not contain r8-Ge [7,14,17], so friction during LHT might prevent the formation of r8-Ge under $\Delta P = 0$ mN compared with $\Delta P = 2$ mN even though the phase transformation to r8-Ge was still dominant compared to other higher ΔP . However, there may well be other explanations for the lower r8-Ge probability for the 0 mN LHT case, and further experiments would be needed to resolve this issue.

Although the positive effect of double cyclic indentation for promoting phase transformation is explained above by referring to the case of Si, the negative effect of increasing residual holding load should be explained in a different way from Si because a high residual load over 10 mN also promotes phase transformation for Si [21,22]. For Ge, two different mechanisms to prevent the formation of r8-Ge might be expected to occur such as nucleation of defects or phase transformation to other phases. A recent indentation study of Si with maximum load held for long times indicated that longer holding time could promote either of defect nucleation or phase transformation [29]. Similar phenomena to this previous study possibly occurred during LHT in the current study. For Ge, defect nucleation is more dominant under slow indentation of dc-Ge [8,14] which is similar to the case of LHT. So, more defects could be nucleated in non-transformed dc-Ge underneath the indenter tip during the LHT process for the case of higher ΔP . Phase transformation and defect nucleation are competitive [10,29], so expansion of the defect nucleated region means a reduction of the transformed region at the second cycle. Therefore, higher ΔP could prevent additional phase transformation during the second cycle, which could be a reason for lower detection fraction of r8-Ge under higher ΔP . On the other hand, in the region which had transformed at the first cycle, accumulation of shear pressure is expected to occur under high ΔP because of separation between phase transformation and defect nucleation regions. Under a high shear and strain condition, phase transformation to st12-Ge may become more probable [7,14,17], so the detection fraction of phase transformation to r8-Ge would decrease, even being less than that for a single indentation. However, the first explanation, that of defect nucleation during the LHT process, is expected to be more likely than st12-Ge formation.

To further verify this explanation, the indentation displacement at the beginning of the second cycle unloading and the residual displacement after the second cycle as shown in Figure 7a were statistically analyzed, and the results are presented in Figure 7b,c respectively. It is noted that even though the indentation displacement at the beginning of the second cycle unloading is almost the same with only a few nm difference as shown in Figure 7b, the residual displacement after the second cycle in Figure 7c gradually decreases with increasing ΔP except that of 0 mN which might contain some error due to re-contact as mentioned above. This is assumed to be caused by lattice volume differences. Relative volume of r8-Ge is ~10% smaller than that of dc-Ge [30]. This implies that dc-Ge with defect nucleation results in a larger difference in volume than that of the denser r8-Ge phase. Such a volume change caused by phase transformation was previously indicated in a DAC experiment [31]. This is consistent to our expectation that the dominant end phase shifted to dc-Ge with defects from r8-Ge with increasing ΔP , leading to smaller indentation displacement after the second cycle as shown in Figure 7c because of larger relative volume of dc-Ge end phase than r8-Ge.

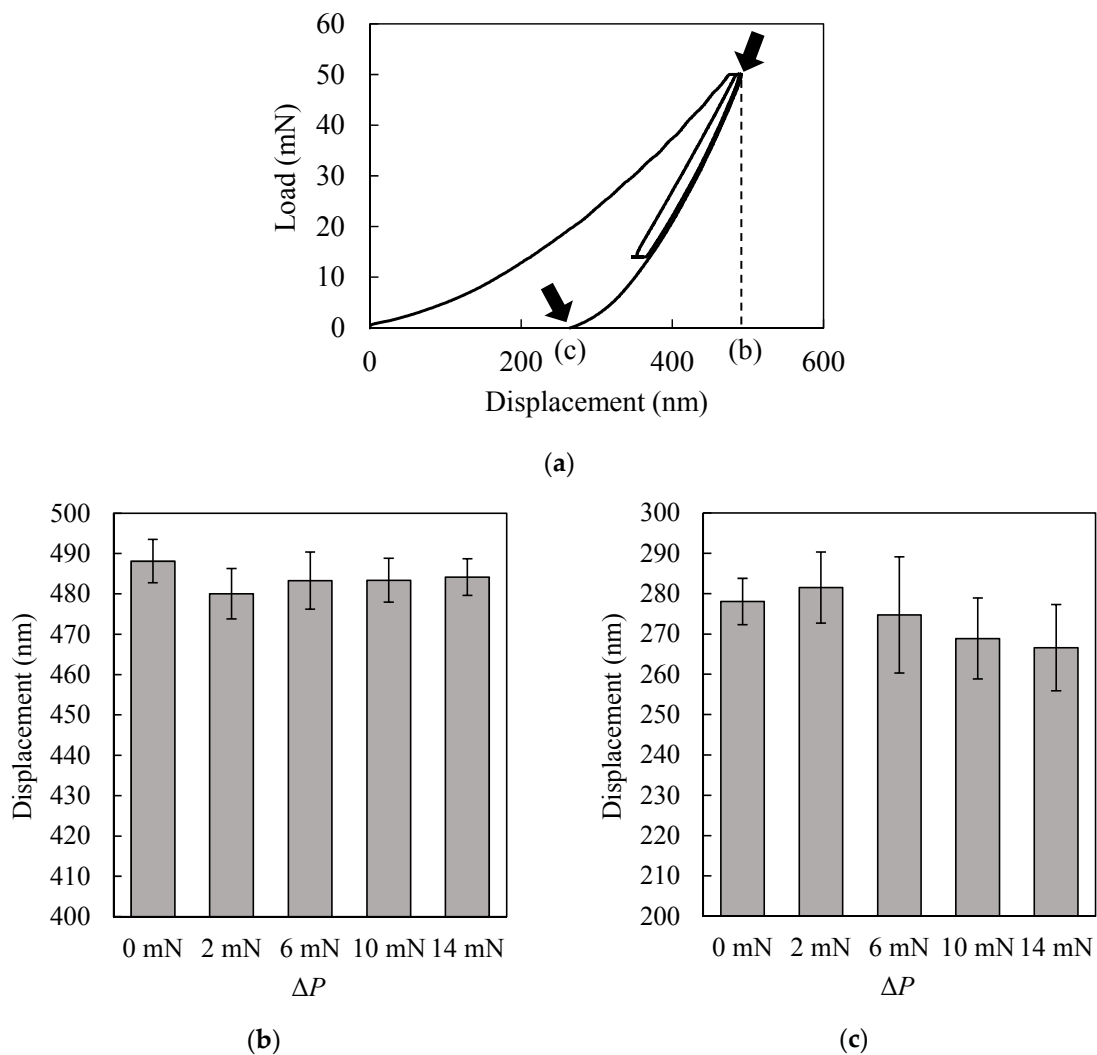


Figure 7. (a) An example of indentation load-displacement curve obtained under double cyclic indentation (real data without artificial shift); (b) the indentation displacement of the beginning of the second cycle unloading; (c) the indentation displacement after the second cycle.

According to the analysis mentioned above, possible phase transformation pathways during double cyclic nanoindentation corresponding to low and high residual loads are illustrated in Figure 8a,b, respectively. During loading of the first cycle, typical phase transformation to $(\beta\text{-Sn})\text{-Ge}$ [1–4] and defect nucleation in the non-transformed region [8,10,14] occurs. After unloading of the first cycle, the transformed region is a mixture of $(\beta\text{-Sn})\text{-Ge}$ and other transformed phases [5–11]. For the case of low residual load in Figure 8a, there is little defect nucleation in the surrounding region and little shear accumulation in transformed region during LHT. This enables phase transformation to r8-Ge during the second cycle and a larger transformed region than a single indentation. As a result, r8-Ge is more frequently detected as the end phase. On the other hand, high residual load causes much defect nucleation and shear accumulation as shown in Figure 8b, which limits the extension of the transformed region during the second cycle. In addition, the accumulated shear results in more defective dc-Ge than r8-Ge. These processes lead to less formation of r8-Ge.

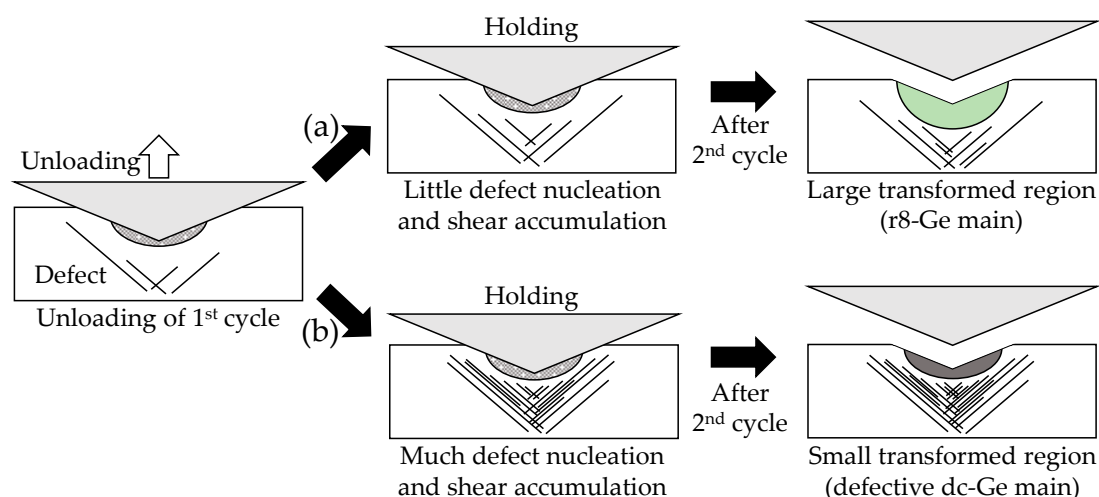


Figure 8. Possible phase transformation pathways during double cyclic nanoindentation: (a) case of low residual load during LHP; (b) case of high residual load during LHP.

4. Conclusions

Phase transformation behaviors in single-crystal Ge were comparatively investigated under single and double cyclic nanoindentation tests. The experimental results indicated that fast double cyclic indentation with low holding residual load remarkably promoted phase transformation from dc-Ge to r8-Ge regardless of the fact that deformation responses were different from single indentation. However, the occurrence of phase transformation decreased with increase in the residual load between the 1st and 2nd cycle. The possible reason is that, although fast and double cyclic indentation with low residual load expands the transformed r8-Ge region by repetitive loading and unloading, the high residual load prevents the expansion of transformed region by further defect nucleation and accumulation of shear which promote more phase transformation to another phase than r8-Ge. This study is expected to give new insights into high pressure phase transformation mechanisms in single-crystal Ge.

Acknowledgments: This research presentation is supported in part by a research assistantship of a Grant-in-Aid to the Program for Leading Graduate School for “Science for Development of Super Mature Society” from the Ministry of Education, Culture, Sport, Science, and Technology in Japan.

Author Contributions: Koji Kosai and Hu Huang conceived and designed the experiments; Koji Kosai performed the experiments; Koji Kosai and Hu Huang analyzed the data; Koji Kosai wrote the paper; Hu Huang and Jiwang Yan supervised the whole study and revised the paper.

Conflicts of Interest: The authors declare no conflict of interest.

References

1. Jamieson, J.C. Crystal Structures at High Pressures of Metallic Modifications of Silicon and Germanium. *Science* **1963**, *139*, 762–764. [[CrossRef](#)] [[PubMed](#)]
2. Minomura, S.; Drickamer, H.G. Pressure Induced Phase Transitions in Silicon, Germanium and Some III–V Compounds. *J. Phys. Chem. Solids* **1962**, *23*, 451–456. [[CrossRef](#)]
3. Gerk, A.P.; Tabor, D. Indentation Hardness and Semiconductor–Metal Transition of Germanium and Silicon. *Nature* **1978**, *271*, 732–733. [[CrossRef](#)]
4. Pharr, G.M.; Oliver, W.C.; Cook, P.F.; Kirchner, P.D.; Kroll, M.C.; Dinger, T.R.; Clarke, D.R. Electrical Resistance of Metallic Contacts on Silicon and Germanium during Indentation. *J. Mater. Res.* **1992**, *7*, 961–972. [[CrossRef](#)]
5. Nelmes, R.J.; McMahon, M.I.; Wright, N.G.; Allan, D.R.; Loveday, J.S. Stability and Crystal Structure of BC8 Germanium. *Phys. Rev. B* **1993**, *48*, 9883–9886. [[CrossRef](#)]

6. Kailer, A.; Nickel, K.G.; Gogotsi, Y.G. Raman Microspectroscopy of Nanocrystalline and Amorphous Phases in Hardness Indentations. *J. Raman Spectrosc.* **1999**, *30*, 939–946. [[CrossRef](#)]
7. Haberl, B.; Guthrie, M.; Malone, B.D.; Smith, J.S.; Sinogeikin, S.V.; Cohen, M.L.; Williams, J.S.; Shen, G.; Bradby, J.E. Controlled Formation of Metastable Germanium Polymorphs. *Phys. Rev. B* **2014**, *89*, 1–6. [[CrossRef](#)]
8. Oliver, D.J.; Bradby, J.E.; Williams, J.S.; Swain, M.V.; Munroe, P. Rate-Dependent Phase Transformations in Nanoindented Germanium. *J. Appl. Phys.* **2009**, *105*, 1–3. [[CrossRef](#)]
9. Johnson, B.C.; Haberl, B.; Deshmukh, S.; Malone, B.D.; Cohen, M.L.; McCallum, J.C.; Williams, J.S.; Bradby, J.E. Evidence for the R8 Phase of Germanium. *Phys. Rev. Lett.* **2013**, *110*, 1–5. [[CrossRef](#)] [[PubMed](#)]
10. Huston, L.Q.; Kiran, M.S.R.N.; Smillie, L.A.; Williams, J.S.; Bradby, J.E. Cold Nanoindentation of Germanium. *Appl. Phys. Lett.* **2017**, *111*, 1–4. [[CrossRef](#)]
11. Jang, J.; Lance, M.J.; Wen, S.; Pharr, G.M. Evidence for Nanoindentation-Induced Phase Transformations in Germanium. *Appl. Phys. Lett.* **2005**, *86*, 1–3. [[CrossRef](#)]
12. Xiao, S.Q.; Pirouz, P. On Diamond-Hexagonal Germanium. *J. Mater. Res.* **1992**, *7*, 1406–1412. [[CrossRef](#)]
13. Williams, J.S.; Haberl, B.; Deshmukh, S.; Johnson, B.C.; Malone, B.D.; Cohen, M.L.; Bradby, J.E. Hexagonal Germanium Formed via a Pressure-Induced Phase Transformation of Amorphous Germanium under Controlled Nanoindentation. *Phys. Status Solidi Rapid Res. Lett.* **2013**, *7*, 355–359. [[CrossRef](#)]
14. Bradby, J.E.; Williams, J.S.; Wong-Leung, J.; Swain, M.V.; Munroe, P. Nanoindentation-Induced Deformation of Ge. *Appl. Phys. Lett.* **2002**, *80*, 2651–2653. [[CrossRef](#)]
15. Deshmukh, S.; Haberl, B.; Ruffell, S.; Munroe, P.; Williams, J.S.; Bradby, J.E. Phase Transformation Pathways in Amorphous Germanium under Indentation Pressure. *J. Appl. Phys.* **2014**, *115*, 1–10. [[CrossRef](#)]
16. Oliver, D.J.; Bradby, J.E.; Ruffell, S.; Williams, J.S.; Munroe, P. Nanoindentation-Induced Phase Transformation in Relaxed and Unrelaxed Ion-Implanted Amorphous Germanium. *J. Appl. Phys.* **2009**, *106*, 1–6. [[CrossRef](#)]
17. Patriarche, G.; Le Bourhis, E.; Khayyat, M.M.O.; Chaudhri, M.M. Indentation-Induced Crystallization and Phase Transformation of Amorphous Germanium. *J. Appl. Phys.* **2004**, *96*, 1464–1468. [[CrossRef](#)]
18. Clarke, D.R.; Kroll, M.C.; Kirchner, P.D.; Cook, R.F.; Hockey, B.J. Amorphization and Conductivity of Silicon and Germanium Induced by Indentation. *Phys. Rev. Lett.* **1988**, *60*, 2156–2159. [[CrossRef](#)] [[PubMed](#)]
19. Haberl, B.; Aji, L.B.B.; Williams, J.S.; Bradby, J.E. The Indentation Hardness of Silicon Measured by Instrumented Indentation: What does It Mean? *J. Mater. Res.* **2012**, *27*, 3066–3072. [[CrossRef](#)]
20. Huang, H.; Yan, J. On the Mechanism of Secondary Pop-Out in Cyclic Nanoindentation of Single-Crystal Silicon. *J. Mater. Res.* **2015**, *30*, 1861–1868. [[CrossRef](#)]
21. Huang, H.; Yan, J. New Insights into Phase Transformations in Single Crystal Silicon by Controlled Cyclic Nanoindentation. *Scr. Mater.* **2015**, *102*, 35–38. [[CrossRef](#)]
22. Huang, H.; Yan, J. Volumetric and Timescale Analysis of Phase Transformation in Single-Crystal Silicon during Nanoindentation. *Appl. Phys. A* **2016**, *122*, 1–11. [[CrossRef](#)]
23. Gogotsi, Y.G.; Domnich, V.; Dub, S.N.; Kailer, A.; Nickel, K.G. Cyclic Nanoindentation and Raman Microspectroscopy Study of Phase Transformations in Semiconductors. *J. Mater. Res.* **2000**, *15*, 871–879. [[CrossRef](#)]
24. Jian, S.R.; Chen, G.J.; Juang, J.Y. Nanoindentation-Induced Phase Transformation in (1 1 0)-Oriented Si Single-Crystals. *Curr. Opin. Solid State Mater. Sci.* **2010**, *14*, 69–74. [[CrossRef](#)]
25. Bradby, J.E.; Williams, J.S.; Wong-Leung, J.; Swain, M.V.; Munroe, P. Transmission Electron Microscopy Observation of Deformation Microstructure under Spherical Indentation in Silicon. *Appl. Phys. Lett.* **2000**, *77*, 3749–3751. [[CrossRef](#)]
26. Haq, A.J.; Munroe, P.R. Phase Transformations in (111) Si after Spherical Indentation. *J. Mater. Res.* **2009**, *24*, 1967–1975. [[CrossRef](#)]
27. Bradby, J.E.; Williams, J.S.; Wong-Leung, J.; Swain, M.V.; Munroe, P. Mechanical Deformation in Silicon by Micro-Indentation. *J. Mater. Res.* **2001**, *16*, 1500–1507. [[CrossRef](#)]
28. Domnich, V.; Gogotsi, Y.; Dub, S. Effect of Phase Transformations on the Shape of the Unloading Curve in the Nanoindentation of Silicon. *Appl. Phys. Lett.* **2000**, *76*, 2214–2216. [[CrossRef](#)]
29. Wang, S.; Haberl, B.; Williams, J.S.; Bradby, J.E. The Influence of Hold Time on the Onset of Plastic Deformation in Silicon. *J. Appl. Phys.* **2015**, *118*, 1–6. [[CrossRef](#)]

30. Malone, B.D.; Cohen, M.L. Electronic Structure, Equation of State, and Lattice Dynamics of Low-Pressure Ge Polymorphs. *Phys. Rev. B* **2012**, *86*, 1–7. [[CrossRef](#)]
31. Menoni, C.S.; Hu, J.Z.; Spain, I.L. Germanium at High Pressures. *Phys. Rev. B* **1986**, *34*, 362–368. [[CrossRef](#)]



© 2017 by the authors. Licensee MDPI, Basel, Switzerland. This article is an open access article distributed under the terms and conditions of the Creative Commons Attribution (CC BY) license (<http://creativecommons.org/licenses/by/4.0/>).